J Biosci (2019) 44:90
DOI: 10.1007/s12038-019-9912-4

Effect of ions and inhibitors on the catalytic activity and structural stability of *S. aureus* enolase

Vijay Hemmadi[1], Avijit Das[1], Om Prakash Chouhan[2], Sumit Biswas[2] and Malabika Biswas[1]*

[1]*Department of Biological Sciences, BITS Pilani, K. K. Birla Goa Campus, NH17B, Zuarinagar, Goa 403726, India*

[2]*VISTA Lab, BITS Pilani, K. K. Birla Goa Campus, Zuarinagar, Goa, India*

**Corresponding author (Email, mbiswas@goa.bits-pilani.ac.in)*

MS received 24 September 2018; accepted 3 May 2019; published online 5 August 2019

The glycolytic enzyme enolase of *Staphylococcus aureus* is a highly conserved enzyme which binds to human plasminogen thereby aiding the infection process. The cloning, over expression and purification of *S. aureus* enolase as well as the effect of various metals upon the catalytic activity and structural stability of the enzyme have been reported. The recombinant enzyme (rSaeno) has been purified to homogeneity in abundant amounts (60 mg/L of culture) and the kinetic parameters (K_m = 0.23 ± 0.013 × 10^{-3} M; V_{max} = 90.98 ± 0.00052 U/mg) and the optimum pH were calculated. This communication further reports that increasing concentrations of Na^+ ions inhibit the enzyme while increasing concentrations of K^+ ions were stimulatory. In case of divalent cations, it was found that Mg^{2+} stimulates the activity of rSaeno while the rest of the divalent cations (Zn^{2+}, Mn^{2+}, Fe^{2+}, Cu^{2+}, Ni^{2+} and Ca^{2+}) lead to a dose-dependent loss in the activity with a total loss of activity in the presence of Hg^{2+} and Cr^{2+}. The circular dichroism data indicate that other than Hg^{2+}, Ni^{2+} and to a certain extent Cu^{2+}, none of the other ions destabilized rSaeno. The inhibitory roles of fluorides, as well as neurotoxic compounds upon the catalytic activity of rSaeno, have also been studied. Conformational changes in rSaeno (induced by ions) were studied using partial trypsin digestion.

Keywords. Catalysis; inhibitor; kinetics; metals; proteolytic; enolase

Abbreviations: BCIP, 5-bromo-4-chloro-3-indolyl phosphate; *E. coli*, *Escherichia coli*; IPTG, isopropyl β-D-1-thiogalactopyranoside; NBT, nitroblue tetrazolium; Ni-NTA, nickel-nitrilotriacetic acid; PEP, phosphoenolpyruvate; PVDF, polyvinylidene difluoride; rSaeno, hexa-histidine tagged *S. aureus* enolase; *S. aureus*, *Staphylococcus aureus*; 2-PGA, 2-phospho-D-glycerate; 6× His-tag, hexa-histidine Tag

1. Introduction

Staphylococcus aureus, a Gram-positive bacterium, is the causal agent of nosocomial as well as community-acquired infections in humans (Steinberg *et al.* 1996). The spectrum of infections ranges from mild skin infections such as boils to life-threatening diseases such as toxic shock syndrome. The problem is further compounded by the emergence of multi-drug resistant *S. aureus* such as methicillin-resistant *S. aureus* and vancomycin-resistant *S. aureus* (Chambers 2001; Proctor 2012). This necessitates the development of alternative therapeutics against the pathogen. A staphylococcal protein which can actually interact with the host and aid in the infection process can thus serve as a potential target for new therapeutics. In this regard, the staphylococcal enzyme enolase appears to be a promising candidate. It has already been reported that *S. aureus* expresses enolase at the surface of its cell wall. Enolase further functions as a receptor for host plasminogen and enhances the staphylokinase activation of plasminogen (Pancholi 2001). Further studies also report that enolase binds to the host laminin thereby enabling the adherence of *S. aureus* to the host cells. This is followed by the activation of host plasminogen and the degradation of laminin which furthers the infection process (Carneiro *et al.* 2004).

Enolase (phosphopyruvate hydratase, EC 4.2.1.11) is involved in the interconversion of 2-phosphoglycerate (2-PGA) and phosphoenolpyruvate (PEP). It is an Mg^{2+}-dependent enzyme and exists as a dimer in most organisms (Wold 1971). However, in a handful of organisms such as *Lactobacillus gasseri*, *Streptococcus pneumoniae*, *Streptococcus suis*, etc.,

Electronic supplementary material: The online version of this article (https://doi.org/10.1007/s12038-019-9912-4) contains supplementary material, which is available to authorized users.

the enzyme exists as an octamer (Barnes and Stcllwagen 1973; Brown *et al.* 1998; Ehinger *et al.* 2004; Lu *et al.* 2012; Raghunathan *et al.* 2014). The interesting feature of *S. aureus* enolase is the fact that the enzyme exists as a dimer as well as an octamer in solution, with the octameric form being the catalytically active form (Wu *et al.* 2015).

Despite the moonlighting functions of *S. aureus* enolase, there are no reports stating the effects of various metal ions and inhibitors on the activity of the enzyme. Thus, to address questions pertaining to the structural stability and catalytic activity of *S. aureus* enolase under the influence of various ions, the *enolase* gene has been cloned, overexpressed and purified as a histidine-tagged recombinant (rSaeno) and the effects of various cations on its structure and function have been studied. The effects of fluoride and neurotoxins on rSaeno have also been studied and reported in this communication.

2. Materials and methods

2.1 *Materials*

Plasmid pET 28a from Novagen (Madison, Wisconsin, USA) was employed for overexpression of enolase. DNA polymerase, restriction enzymes and T4 DNA ligase were procured from Fermentas GmbH (Germany). The cloning host *Escherichia coli* DH5α and expression host *E. coli* BL21 (DE3) were obtained from Novagen (Madison, Wisconsin, USA). Ni^{2+}-nitrilotriacetic acid (Ni-NTA) agarose resin was procured from Thermo Scientific (USA). Polyvinylidene difluoride (PVDF) membrane, isopropyl β-D-1-thiogalactopyranoside (IPTG) and antibiotics were obtained from Sigma (St. Louis, MO, USA). Anti-His antibody, anti-mouse IgG (H+L) alkaline phosphatase conjugate, 5-bromo-4-chloro-3-indolyl phosphate (BCIP)/nitroblue tetrazolium (NBT) colour development substrate, Dithiothreitol (DTT) and Bradford reagents were purchased from Bio-Rad (CA, USA). The enolase substrate PEP was obtained from Sigma-Aldrich Co. The chemicals used in this study were of reagent grade from Sigma Chemical Co. (MO, USA).

2.2 *Staphylococcus strain and culture conditions*

S. aureus RN4220 was grown in Trypticase soy broth at 37°C (Lee and Iandolo 1988). *E. coli* DH5α cells and *E. coli* BL21 (DE3) were grown in Luria-Bertani (LB) broth at 37°C (Sambrook *et al.* 1989). The growth media were supplemented with appropriate antibiotics (kanamycin 25 μg/μL).

2.3 *Cloning, and overexpression of recombinant enolase (rSaeno)*

Genomic DNA from *S. aureus* was extracted and purified according to the method of Zhao *et al.* (2012). The *enolase* gene of *S. aureus* was polymerase chain reaction (PCR) amplified from the isolated genomic DNA using *DreamTaq* DNA polymerase (Fermentas) and the following set of primers: enolase-F: 5′-CATATGCCAATTATTACAGATG TTTACGCTC-3′ and enolase-R: 5′-CTCGAGTTATTTAT CTAAGTTATAGAATGATTTGATACCG-3′. The PCR reaction was carried out in a T100™ Thermal cycler (Bio-Rad, USA). The amplified PCR product of 1305 bp as well as pET28a overexpression vector were digested with NdeI and XhoI and further ligated with T4 DNA ligase.

The ligation mixture was transformed into freshly prepared *E. coli* DH5α competent cells. The recombinants were screened by plasmid DNA preparation followed by restriction enzyme digestion. A healthy recombinant was selected and sequenced (CIF, UDSC) and designated as prSaeno. prSaeno was transformed into competent *E. coli* BL21 (DE3) cells. Thereafter, a healthy transformant was selected and used for all other experiments.

Hexa-histidine tagged *S. aureus* enolase (designated as rSaeno) was overexpressed by the addition of 0.5 mM IPTG to an *E. coli* (carrying prSaeno) cell culture in the log phase. Cells were further cultured in a shaking incubator at 140 rpm at 32°C for 3 h. Protein purification was carried out at 4°C. The induced cells were harvested by centrifugation at 6500 rpm for 10 min at 4°C and resuspended in buffer A (20 mM Tris-HCl, pH 8.0, 500 mM NaCl and 5% glycerol and 10 mM imidazole) followed by sonication. The sonicated cell extract was centrifuged at 10,000 rpm for 30 min at 4°C.

2.4 *Purification of rSaeno by affinity chromatography and dialysis*

rSaeno was purified from the soluble cellular fractions by Ni-NTA acid affinity chromatography according to the manufacturer's protocol (Thermo Scientific, USA). The binding was accomplished by the batch method. Initially, the Ni-NTA column was pre-equilibrated with pre-equilibration buffer (20 mM Tris-HCl, pH 8.0, 500 mM NaCl and 10 mM imidazole) for 15 min. The soluble cellular extract was then allowed to interact with Ni-NTA (10 mL/L of culture) for 1 h in four cycles with a 15 min interval. The column was washed with 50-bed volumes of wash buffer (20 mM Tris-HCl, pH 8.0, 500 mM NaCl, 25 mM imidazole and 5% glycerol) to remove the non-specifically bound *E. coli* proteins from the column. rSaeno was then eluted with elution buffer (20 mM Tris-HCl, pH 8.0, 100 mM NaCl, 300 mM imidazole and 5% glycerol). Before carrying out further experiments, the purified rSaeno was dialysed thoroughly in dialysis buffer (20 mM Tris-HCl pH 8.0, 200 mM NaCl, 5% glycerol and 1 mM Ethylenediaminetetraacetic acid (EDTA)) (Pal-Bhowmick *et al.* 2004).

2.5 *Qualitative and quantitative analysis and kinetic characterization of rSaeno*

Purified rSaeno was quantified by the Bradford reagent and was qualitatively analysed by SDS-10% PAGE followed by

western blotting according to the standard procedures (Amersham Bioscience, UK) (supplementary figure 1). In brief, the gel was blotted on a PVDF membrane at 50 V for 30 min at 4°C in transfer buffer (25 mM Tris and 192 mM glycine). The mouse anti-His antibody (1:500) was utilized as a primary antibody and the anti-mouse IgG alkaline phosphatase conjugated antibody (1:7500) was employed as a secondary antibody. BCIP and NBT served as substrates (Pal-Bhowmick *et al.* 2004; Agarwal *et al.* 2008).

To study the activity of purified rSaeno, the conversion of PEP into 2-PGA by the purified protein was monitored. The experiment was carried out at 25 ± 1°C. Briefly, the decrease in absorbance (due to the formation of PGA) at 240 nm for 15 min at 1 s intervals (UV-24050, UV–visible spectrophotometer with equibath) was spectrophotometrically monitored. The molar extinction coefficient of PEP was 1.1×10^{-3}/M/cm. The assay mixture consisted of 20 mM Tris-HCl (pH 7.5), 400 mM KCl, 1 mM $MgSO_4$, 15 nM rSaeno and varying concentrations of PEP (0.1–3 mM) in a total volume of 200 µL (Wu *et al.* 2015). One unit of enzyme was defined as the amount of rSaeno that converts 1 µmol of PEP into 2-PGA in 1 min at 25°C. The initial velocity was calculated from the slope of the linear progression curve of 60 s duration. The kinetic coefficients K_m, V_{max}, k_{cat} and k_{cat}/K_m were calculated from the Michaelis–Menten plot using GraphPad Prism software of version 6.01 (Pal-Bhowmick *et al.* 2004; Wu *et al.* 2015).

2.6 *Effect of monovalent cations on rSaeno activity*

To elucidate the effect of monovalent cations, rSaeno was treated with sodium chloride or potassium chloride. The assay buffer consisted of 20 mM Tris-HCl (pH 7.5), 1 mM $MgSO_4$ and 15 nM rSaeno with various concentrations of NaCl or KCl (0–600 mM). The reaction was initiated by the addition of 2 mM PEP. All reactions were performed at 25 ± 1°C (Agarwal *et al.* 2008).

2.7 *Effects of divalent cations on rSaeno activity*

To study the effect of divalent cations, the standard rSaeno reaction was utilized. The assay buffer consisted of 20 mM Tris-HCl buffer (pH 7.5) supplemented with 400 mM KCl and 15 nM rSaeno; contrary to the standard method, 1 mM $MgSO_4$ was replaced with 1 mM sulphates of various divalent cations (Zn^{2+}, Mn^{2+}, Cu^{2+}, Ni^{2+}, Ca^{2+} and Hg^{2+}).

In each case, the reaction was initiated by the addition of 2 mM PEP to the final volume of 200 µL at 25 ± 1°C. The decrease in the absorbance of PEP at 240 nm was monitored for 15 min at 1 s intervals (Brewer 1985; Lee *et al.* 2006; Han *et al.* 2012).

2.8 *pH-Dependent activation of rSaeno by Mg^{2+}, Zn^{2+} and Mn^{2+} ions*

The optimum concentration of Mg^{2+}, Zn^{2+} and Mn^{2+} required for maximum catalytic activity of rSaeno was determined by varying the concentration of these cations from 0 to 5 mM in the standard assay buffer (400 mM KCl, 15 nM rSaeno and 2 mM PEP) with the pH ranging from 4 to 10 at 25 ± 1°C. The decrease in the absorbance of PEP at 240 nm was monitored for 15 min at 1 s intervals (Vinarov and Nowak 1998).

2.9 *Effect of neurotoxins on the catalytic activity of rSaeno*

2.9.1 *Inhibition of rSaeno by acrylamide:* Equal volumes of rSaeno (15 nM) and acrylamide (15 nM) were incubated in Tris-HCl (pH 7.5) for 30 min at 25 ± 1°C in a shaking water bath. At the end of this incubation, 400 mM KCl and 1 mM $MgSO_4$ were added to the reaction mixture. The reaction was then initiated by the addition of PEP (0–3 mM). The decrease in the absorbance of PEP at 240 nm was monitored for 15 min at 1 s intervals at 25 ± 1°C. The kinetic coefficients K_m and V_{max} were calculated from Michaelis–Menten plot.

To determine the reversibility of acrylamide inhibition, equal volumes of rSaeno (15 nM) and acrylamide (15 nM) were incubated in Tris-HCl of pH 7.5 for 30 min at 25 ± 1°C in a shaking water bath. The rSaeno–acrylamide complex thus formed was dialysed overnight at 4°C, in dialysis buffer (20 mM Tris, pH 8, 200 mM NaCl, 5% glycerol and 1 mM EDTA). The dialysed rSaeno was assayed for its activity by the addition of 400 mM KCl, 1 mM $MgSO_4$ and PEP (0–3 mM). The activity was measured at 240 nm for 15 min at 1 s intervals at 25 ± 1°C. The kinetic parameters were calculated.

The effect of sulphhydryl agent on acrylamide inhibition was also analysed. In this case, equal volumes of rSaeno (15 nM) and acrylamide (15 nM) were incubated in Tris-HCl of pH 7.5 in the presence of DTT (0–10 mM). The incubation was carried out for 30 min at 25 ± 1°C in a shaking water bath following which 400 mM KCl and 1 mM $MgSO_4$ were added to the reaction mixture. The reaction was then initiated by the addition of PEP (2 mM). To determine the reversibility of inhibition, the acrylamide, enolase and DTT complexes were dialysed in the above-mentioned dialysis buffer. After dialysis, the activity of enolase was monitored at 25 ± 1°C at 240 nm for 15 min at 1 s intervals.

To study the impact of cations on acrylamide inhibition of rSaeno, 15 nM rSaeno was preincubated with varying concentrations of magnesium, manganese and zinc (0.05–5 mM) individually in Tris-HCl of pH 7.5 for 15 min at 25 ± 1°C in a shaking water bath. At the end of the incubation, 15 nM acrylamide was added to the mixture

which was further incubated for 30 min at 25 ± 1°C in a shaking water bath. This was followed by the addition of 400 mM KCl and 2 mM PEP. The decrease in the absorbance of PEP at 240 nm was monitored at 25 ± 1°C for 15 min at 1 s intervals (Howland *et al.* 1980).

2.9.2 *Inhibition of rSaeno by 2,5-hexanedione:* rSaeno (15 nM) was incubated with 2,5-hexanedione (0–10 mM) in 20 mM Tris-HCl (pH 7.5) for 30 min at 25 ± 1°C in a shaking water bath. This was followed by the addition of 400 mM KCl and 1 mM $MgSO_4$ to the above reaction mixture. The reaction was initiated by the addition of 2 mM PEP and the decrease in the absorbance of PEP at 240 nm was monitored at 25 ± 1°C for 15 min at 1 s intervals

The reversibility of the inhibition was assayed by dialysing the rSaeno-2,5-hexanedione complex in dialysis buffer (mentioned above) and then assaying for rSaeno activity. The 2,5-hexanedione inhibition was also carried out in different concentrations (0–5 mM) of magnesium, manganese and zinc to elucidate the impact of divalent cations on 2,5-hexanedione inhibition of rSaeno (Howland *et al.* 1980).

2.10 *Fluoride inhibition*

The standard assay mixture (20 mM Tris-HCl (pH 7.5), 400 mM KCl, 1 mM $MgSO_4$ and 15 nM rSaeno) was prepared. To this, varying concentrations (0–5 mM) of sodium fluorophosphate (Na_2FPO_3), sodium fluoride (NaF), calcium fluoride (CaF_2), potassium fluoride (KF) and ammonium fluoride (NH_4F) were added individually. The reaction was initiated by the addition of 2 mM PEP and the decrease in the absorbance of PEP at 240 nm was monitored at 25 ± 1°C for 15 min at 1 s intervals.

The effect of cations on fluoride inhibition of rSaeno was analysed by carrying out sodium fluorophosphate (Na_2FPO_3) (0–5 mM) inhibition of rSaeno in the presence of 1 mM sulphates of magnesium, manganese and zinc (Maurer and Nowak 1981; Curran *et al.* 1994; Belli *et al.* 1995).

2.11 *Circular dichroism (CD) spectral analysis and tryptophan fluorescence measurement of rSaeno in different ions*

rSaeno was pre-incubated with different ions (Mg^{2+}, Zn^{2+}, Mn^{2+}, Cu^{2+}, Ni^{2+}, Ca^{2+} and Hg^{2+}) for 15 min and was subjected to CD analysis (wavelength 200–260 nm, bandwidth 1.00 nm, data pitch 0.5 nm and scanning speed 50 nm/min) by using a JASCO J-815 CD spectrometer (JASCO CD/A029961168, JASCO, Easton, MD, USA) in quartz cells or cuvettes of 1 mm diameter and Reed's reference was used for the estimation of the secondary structure (Sreerama and Woody 2000).

The 3.5 mg/mL rSaeno stock was diluted to 0.040 mg/mL with 20 mM Tris-HCl buffer (pH 7.5) and pre-incubated with divalent cations (1 mM Mg^{2+}, Zn^{2+}, Mn^{2+}, Cu^{2+}, Ni^{2+}, Ca^{2+}, NH_4^+ or Hg^{2+}) as well as with monovalent cations (NaCl (0–600 mM) or KCl (0–600 mM)) individually for 15 min. The intrinsic tryptophan fluorescence was monitored at 25 ± 1°C on a JASCO FP8200 spectrofluorimeter using a 500 µL quartz cuvette with a 4 mm path length. Slits were set to 3 and 5 nm for excitation and emission, respectively. The excitation wavelength was 295 nm and the emission was recorded from 310 to 450 nm with 0.5 nm increments.

2.12 *Partial trypsin digestion*

The limited proteolysis assay was employed to determine the protective effect of Mg^{2+}, Zn^{2+}, Mn^{2+}, Cu^{2+}, Ni^{2+} and Hg^{2+} on enolase. To remove the intrinsic conformational divalent metal ions, metal-free rSaeno was prepared by extensive dialysis of rSaeno at 4°C against 50 mM Tris-HCl buffer (pH 7.5), containing 150 mM NaCl and 5 mM β-mercaptoethanol with four changes of buffer once every 12 h. Further, the complete removal of metals from the dialysed enzyme solution was confirmed by atomic absorption spectrophotometry (AA-7000, Shimadzu Corporation, Japan) (supplementary table 1). The study was divided into two sets. In one set, the metal-free rSaeno (0.5 mg/mL) was incubated with trypsin (0.001 mg/mL) and 2 mM EDTA in 50 mM Tris-HCl buffer of pH 7.5 at 25°C. In the second set, the metal-free rSaeno (0.5 mg/mL) was incubated with trypsin (0.001 mg/mL) and 5 mM Mg^{2+}, Zn^{2+}, Mn^{2+}, Cu^{2+}, Ni^{2+} or Hg^{2+} individually, in 50 mM Tris-HCl buffer of pH 7.5 at 25°C. The metal-free enzyme (in the absence of trypsin) was taken as the control. The aliquots were withdrawn from the reaction mixture at various time intervals. The proteolytic action of trypsin was stopped by the addition of 5× SDS gel loading buffer (50 mM Tris-HCl, pH 6.8, 2% SDS, 5 mM DTT, 0.1% bromophenol blue and 10% glycerol) in a 4:1 ratio and boiled for 2 min in a boiling water bath. The samples were run on SDS-10% PAGE. Undigested protein bands were quantified using ImageJ software. The control band was considered as 100% and digested band intensities were compared with the control (Dutta *et al.* 2015).

3. Results

3.1 *Cloning of the enolase gene from Staphylococcus aureus*

The *enolase* gene was PCR amplified as described in section 2 and a DNA band of 1305 bp was observed (supplementary figure 1) in a 1.0% agarose gel. This band was gel purified, double digested with NdeI and XhoI and ligated into a pET28a vector (double digested with NdeI and XhoI). The ligation mixture was transformed into XL1 blue

competent *E. coli* cells. The transformants that had grown on the LB agar media plates supplemented with kanamycin (25 μg/mL) were screened and selected for the presence of *enolase* gene by PCR using forward and reverse primers (see section 2) of enolase. Five of the transformants were found to be positive and gave a band at 1305 bp (supplementary figure 2) when run on a 1% agarose gel. This cloning incorporated 20 extra amino acids at the N-terminal end of the protein.

3.2 *Overexpression and purification of rSaeno*

The N-terminal hexa-histidine tagged rSaeno was purified to homogeneity from 1.5 L of *E. coli* BL21 (λDE3) carrying prSaeno by immobilized metal affinity chromatography (IMAC). IMAC (Ni^{2+}-NTA) successfully purified rSaeno from clarified cell lysates and the different fractions of washes and elutes were analysed by SDS-12% PAGE (supplementary figure 3). As is clear from the gel (supplementary figure 3), the purified rSaeno migrated as a single band with an apparent molecular mass of 48.18 kDa. rSaeno was detected using western blot as a band of approximately 48.18 kDa (supplementary figure 4).

3.3 *Enzyme kinetic assay of the rSaeno*

The kinetic parameters for the rSaeno were determined for the reverse reaction (conversion of PEP into 2-PGA). A 15 nM of highly purified rSaeno was used with varying concentrations of PEP (0.1–3 mM). rSaeno exhibited standard Michaelis–Menten kinetics for PEP. The kinetic coefficients K_m, V_{max}, k_{cat} and k_{cat}/K_m were calculated from the Michaelis–Menten plot using GraphPad Prism software of version 6.01 (Wu et al. 2015). The rate constants for PEP was $K_m = 0.231 \pm 0.013 \times 10^{-3}$ M, $V_{max} = 90.98 \pm 0.00052$ U/mg, $k_{cat} = 0.72 \times 10^2$/s and $k_{cat}/K_m = 3.12 \times 10^5$/M/s (figure 1).

3.4 *Effect of monovalent cations on the catalytic activity of rSaeno*

The effect of monovalent cations on the catalytic activity of rSaeno was investigated. The changes in the catalytic activity of the enzyme in the presence of varying concentrations of NaCl or KCl are presented in figure 2. From figure 2, it is clear that rSaeno is inhibited by NaCl, even at low concentrations. The catalytic activity of the enzyme is reduced to almost 50% at 0.1–0.2 M concentration of NaCl. KCl, on the other hand, has a stimulatory effect upon the catalytic activity of rSaeno. The enzyme exhibits maximum activity at a 0.45 M concentration of KCl. However, at a higher concentration of KCl (0.5–0.8 M), the enzyme activity decreases by 10–15%.

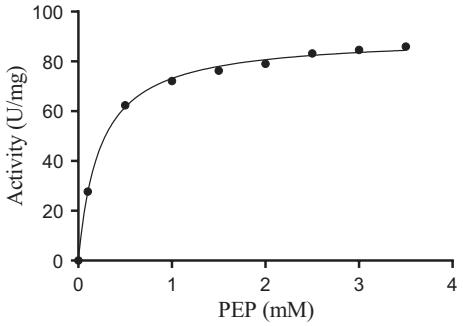

Figure 1. Substrate concentration dependence of enzyme activity. rSaeno activity was measured at different concentrations of PEP varying between 0.1 and 3.0 mM. Data were fitted to the Michaelis–Menten equation using GraphPad. The best-fit values for the kinetic constants obtained were $K_m = 0.231 \pm 0.013 \times 10^{-3}$ M, $V_{max} = 90.98 \pm 0.00052$ U/mg, $k_{cat} = 0.72 \times 10^2$/s and $k_{cat}/K_m = 3.12 \times 10^5$/M/s. Symbols represent measured activity while the curve is the best fit.

3.5 *Effect of divalent cations on the catalytic activity of rSaeno*

To study the effects of different divalent cations upon the catalytic activity of rSaeno, the conversion of PEP into 2-PGA in the presence of 1 mM each of Mg^{2+}, Zn^{2+}, Mn^{2+}, Fe^{2+}, Cu^{2+}, Ni^{2+}, Ca^{2+}, Hg^{2+} or Cr^{2+} was monitored. A comparison of the effects of these divalent cations upon the activity of rSaeno is presented in table 1. The data clearly indicate that the enzyme is strongly activated by Mg^{2+} and Zn^{2+} with Mg^{2+} being the strongest activator. Mn^{2+} and Cu^{2+} have a slight activating effect upon the catalytic activity of rSaeno while Ni^{2+} and Ca^{2+} are very weak activators. A total loss of catalytic activity was observed in the presence of Hg^{2+} (table 1). It has already been reported

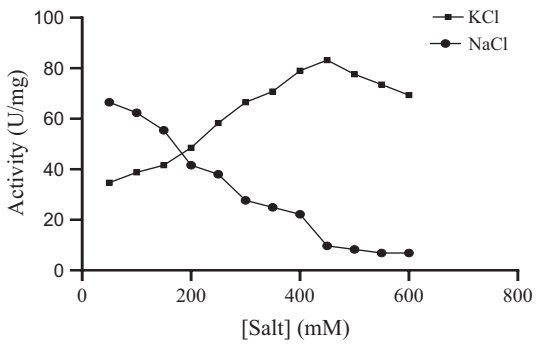

Figure 2. Effect of monovalent cations (NaCl or KCl) on rSaeno activity. The assay buffer consisted of 20 mM Tris-HCl (pH 7.5), 1 mM $MgSO_4$ and 15 nM rSaeno with various concentrations of NaCl or KCl (0–600 mM). The reaction was initiated by the addition of 2 mM PEP. The decrease in the absorbance of PEP at 240 nm was monitored for 15 min at 1 s intervals at 25 ± 1°C. Data were plotted as activity *vs* [salt]. The increase in the concentration of Na^+ ions inhibits the enzyme while increasing concentrations of K^+ ions were stimulatory.

Table 1. rSaeno activity in the presence of 1 mM sulphates of various divalent cations at 25 ± 1°C

Metal ions	Activity of His-Eno (U/mg)	Relative activity (%)
Mg^{2+}	72.11	100
Zn^{2+}	62.40	86.5
Mn^{2+}	45.76	63.4
Fe^{2+}	45.07	62.5
Cu^{2+}	38.83	53.8
Ni^{2+}	24.96	34.6
Ca^{2+}	18.33	25.4
Hg^{2+}	0	0
Cr^{2+}	0	0

In the standard assay buffer (20 mM Tris-HCl buffer, pH 7.5, 400 mM KCl and 15 nM rSaeno), 1 mM $MgSO_4$ was replaced with 1 mM sulphates of various divalent cations (Zn^{2+}, Mn^{2+}, Cu^{2+}, Ni^{2+}, Ca^{2+} and Hg^{2+}). The reaction was initiated by the addition of 2 mM PEP.

that Mg^{2+} ions are essential for the activity of the enzyme (Wold 1971). rSaeno–Cr^{2+} and rSaeno–Hg^{2+} complexes were extensively dialysed to remove Cr^{2+} and Hg^{2+} from rSaeno. The dialysed enzyme was not able to catalyse the conversion of PEP into 2-PGA. This indicates that Cr^{2+} and Hg^{2+} irreversibly inactivated the enzyme.

3.6 *rSaeno activity was inhibited by higher concentrations of divalent cations*

The activity of rSaeno is inhibited by higher concentrations of different divalent cations. While Mg^{2+}, Mn^{2+} and Zn^{2+}, at a lower concentration (1 mM), had an activating effect upon rSaeno, higher concentrations of the same ions inhibited the activity of the enzyme.

The pH of the assay buffer further affected the concentration of the divalent cations required for the maximum activity of rSaeno. The activity of rSaeno was measured in the pH range of 4.0–10.0 with increasing concentrations of Mg^{2+}, Mn^{2+} or Zn^{2+} (0–5 mM). At lower pH values, inhibition in catalytic activity is observed as the concentration of Mg^{2+} was increased to 2 mM and above (figure 3A and D). As the pH is increased to 10, the Mg^{2+}-induced inhibition becomes progressively weaker and the enzyme requires 2 mM Mg^{2+} for maximum activity (figure 3D and E).

Interestingly, the maximum activity of the enzyme was achieved only at higher concentrations of Zn^{2+} (>0–0.5 mM) at all pH values (4, 5, 6, 7, 7.5, 8, 9 and 10). Increasing concentrations of Zn^{2+} conferred significant increments to rSaeno activity; the maximum activity was found to be at pH 7.5 while at pH 7 and 8 there was moderate activity. At pH 4 and 5, rSaeno showed minimum activity even at higher concentrations of Zn^{2+}. The Zn^{2+} optima of rSaeno were found to be totally dependent on pH. The Zn^{2+} optima were 1 mM at low and moderate pH (4, 5, 6, 7, 7.5 and 8) but at higher pH values (9 and 10) the optima shifted from 1 to 2 mM with a subsequent decrease in rSaeno activity (figure 3B–E).

In the case of Mn^{2+}, at pH 7 and 7.5 rSaeno showed maximum activity, and moderate activity was exhibited at pH 8 and 6. But at pH 4 and 5, rSaeno activity was found to be minimum. The influence of pH on Mn^{2+} optima can be clearly observed in the graph (figure 3C). The Mn^{2+} optima were found to be 1.5 mM at pH 7.5, 7, 8 and 6. However, the optima shifted to 2 mM of Mn^{2+} at higher pH ranges such as pH 9 and 10. At lower pH ranges there was a drastic decrease in the rSaeno activity but Mn^{2+} optima were not changed (figure 3C–E) (Brewer 1985).

3.7 *Inhibition of rSaeno by neurotoxins (acrylamide and 2,5-hexanedione)*

3.7.1 *Inhibition of enolase by acrylamide:* To study the inhibition induced by acrylamide on rSaeno, the catalytic activity of the enzyme was monitored in the presence or absence of acrylamide, using varying concentrations of PEP. From the data presented in figure 4 and table 2, it is observed that there is an increase in K_m and a decrease in V_{max} in the presence of acrylamide. This is indicative of the fact that acrylamide induces a mixed type of inhibition (Curran *et al.* 1994)

3.7.2 *The inhibition induced by acrylamide is reversible in nature:* The acrylamide treated rSaeno was extensively dialysed in dialysis buffer to completely remove acrylamide. The catalytic activity of the dialysed rSaeno was then monitored in the presence of various concentrations of PEP. The data presented in figure 4 and table 3 clearly indicate the reversibility of acrylamide inhibition since the activity of the dialysed enzyme was completely restored to the non-inhibited rates.

3.7.3 *Dithiothreitol augments the inhibition of rSaeno induced by acrylamide:* The results of this experiment are presented in figure 5. The results indicate that DTT by itself does not inhibit rSaeno activity. However, the presence of DTT in varying concentrations enhances the inhibition of rSaeno activity induced by acrylamide (figure 10). While induced 15 nM acrylamide alone inhibited rSaeno activity by 33%, the same concentration of the neurotoxin in the presence of 10 mM DTT inhibited 99.81% of enzyme activity.

3.7.4 *2,5-Hexanedione irreversibly inhibited the rSaeno activity:* The preliminary observations confirmed that inhibitory potency of 2,5-hexanedione is independent of pre-incubation of 2,5-hexanedione and rSaeno inhibitory complex. Dose-dependent inhibition of rSaeno by 2,5-hexanedione was observed. To determine the reversibility of inhibition, the 2,5-hexanedione and the rSaeno inhibitory complex were dialysed in dialysis buffer and assayed for activity. The enzyme activity was not rejuvenated even upon dialysis. This implicates that the inhibition of rSaeno activity by 2,5-hexanedione is irreversible in nature (figure 6).

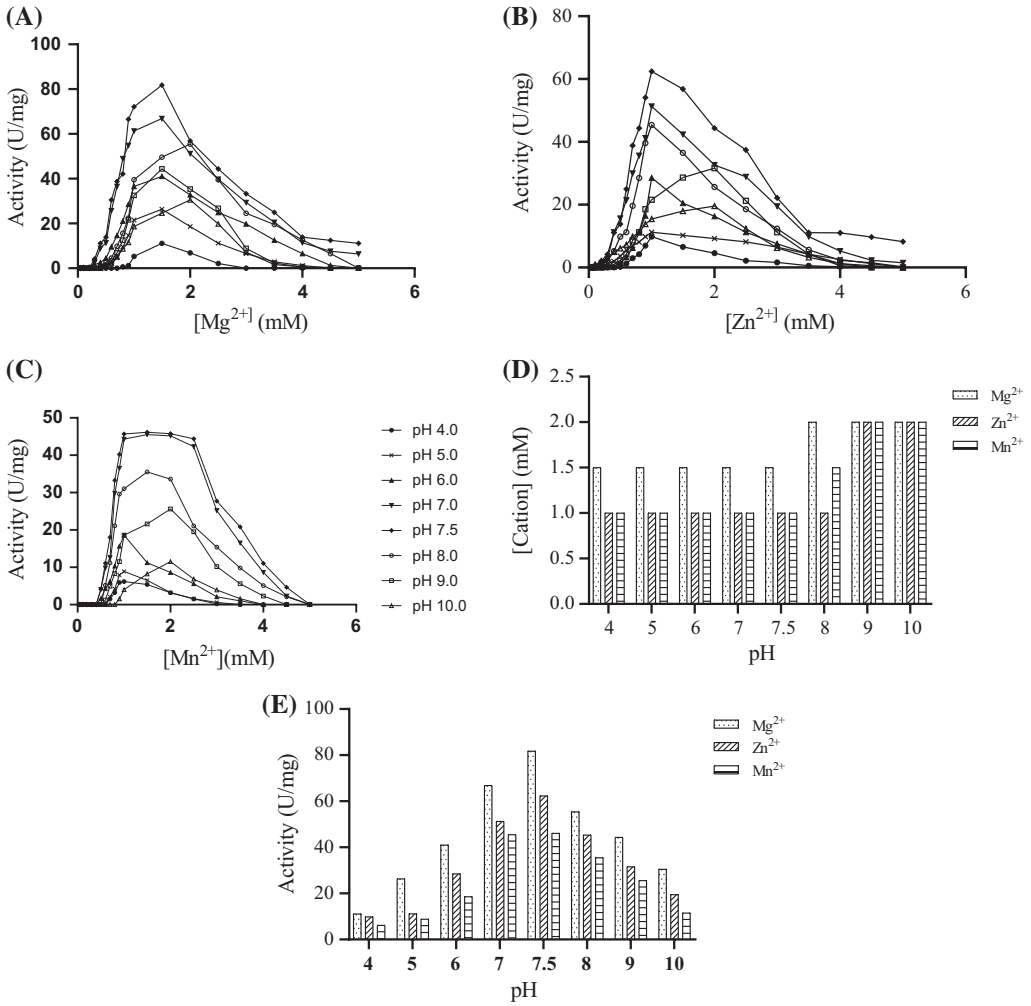

Figure 3. Effect of pH on metal-mediated activation of rSaeno. 15 nM rSaeno activity was measured for varying concentrations (0–5 mM) of (**A**) Mg^{2+} or (**B**) Zn^{2+} or (**C**) Mn^{2+} in the standard assay buffer (400 mM KCl and 2 mM PEP) with pH ranging from 4 to 10 at 25 ± 1°C. The conversion of PEP into 2-PGA was monitored at 240 nm for 15 min at 1 s intervals. (**D**) pH *vs* cation concentrations needed for maximal activity of rSaeno. (**E**) pH *vs* maximal specific activity observed for rSaeno.

3.8 *Sodium fluorophosphate (Na_2FPO_3) is a potent inhibitor of rSaeno*

The effect of fluoride on rSaeno activity was studied by directly incorporating fluoride into the enzyme–substrate system. Among the various fluorides tested, sodium fluorophosphate (K_i = 0.4 mM) significantly inhibited rSaeno more than any other fluorides (figure 7). Other studied fluorides had an inhibitory K_i ranging from 0.6 to 1.8 mM.

3.9 *Effect of metals on enolase inhibition*

In this study, the enzyme was initially preincubated with various divalent cations (Mg^{2+}, Zn^{2+} or Mn^{2+}) and then further incubated with the inhibitors separately (acrylamide, 2,5-hexanedione or sodium fluorophosphate) to elucidate the impact of divalent cations on enolase inhibition. In the acrylamide inhibition, various divalent cations showed various responses. In this juncture, Mg^{2+} conferred the significant protection (23% protection) whereas Zn^{2+} was neutral in inhibition (2% protection). In contrast, Mn^{2+} (14% increment in the inhibition) potentiated the acrylamide inhibition (table 3).

In the presence of 2,5-hexanedione, none of the divalent cations conferred any protection against inhibition. One of the potent cofactors of rSaeno, Mg^{2+}, was neutral in protection. On the other hand, Zn^{2+} and Mn^{2+} potentiated the inhibition. This indicates that metal ions such as Mg^{2+} might impart a certain level of protection against the reversible inhibitor but not for the irreversible inhibitor. And the replacement of Mg^{2+} with less potent cofactors (such as Zn^{2+} or Mn^{2+}) results in either neutral or enhanced inhibition in both the cases of reversible and irreversible inhibition (table 3).

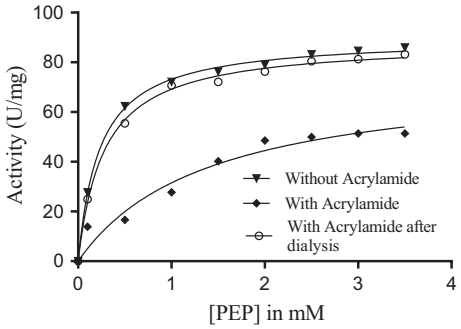

Figure 4. Kinetics of acrylamide inhibition of rSaeno. 15 nM rSaeno was assayed at 240 nm for 15 min at 1 s intervals in the presence (15 nM acrylamide) and absence of acrylamide, using varying concentrations of PEP (0.1–3.0 mM). To determine the reversibility of acrylamide inhibition, the acrylamide–rSaeno complex was extensively dialysed in dialysis buffer to completely remove acrylamide. The dialysed rSaeno was then assayed in standard assay buffer with varying concentrations of PEP (0.1–3.0 mM) at 25 ± 1°C. The kinetic parameters (V_{max} and K_m) were calculated by using the Michaelis–Menten plot.

Table 2. Effect of acrylamide on kinetic characteristics of rSaeno

Enzyme sample	K_m (M)	V_{max} (U/mg)
Without acrylamide	$0.231 \pm 0.013 \times 10^{-3}$	90.98 ± 0.00052
With acrylamide	$1.401 \pm 0.048 \times 10^{-3}$	75.64 ± 0.0061
After dialysis	$0.277 \pm 0.018 \times 10^{-3}$	88.35 ± 0.00023

Enzyme was assayed in the presence of 15 nM acrylamide and also in the absence of acrylamide. It was also assayed after the removal of acrylamide by extensive dialysis. The data are shown in figure 4. Best-fit values for K_m and V_{max} are listed in the table.

In the case of quasi-irreversible (Curran *et al.* 1994) (sodium fluorophosphates) inhibition, the metal ions behaved differently. The rSaeno inhibition by sodium fluorophosphates was high in the presence of the potent cofactor of rSaeno (Mg^{2+}). Interestingly, the inhibitory potential of sodium fluorophosphates was significantly decreased when Mg^{2+} was replaced with Zn^{2+} (20% less inhibition than Mg^{2+}) and Mn^{2+} (30% less inhibition than Mg^{2+}) (table 4).

3.10 *Effects of various ions on the structure of rSaeno*

To further investigate the effect of various ions upon the structure of the rSaeno, CD spectral analysis (200–240 nm) was carried out for the enzyme after incubating it under the desired conditions. The CD spectra of rSaeno in the presence of different metal ions (divalent) indicate the profound effect exerted by metal ions upon the structure of the protein (figure 8, table 5). From figure 8, it is clear that rSaeno exhibited a much-reduced peak at 208 nm in the presence of Ni^{2+} and Hg^{2+} ions, indicating a loss in the alpha-helical content of the protein. More interestingly, table 5 reveals that the protein loses the beta-pleated structure completely in the presence of Cu^{2+}, Ni^{2+} and Hg^{2+} ions, with a concomitant increase in the random coil. In fact, the protein appears to be in a very stable conformation in the presence of Mg^{2+} or Zn^{2+} ions. These observations were also supported by intrinsic tryptophan fluorescence (λ_{ex} at 295 nm) where the variations in the proteins' architecture due to the effect of the metal ions were investigated. It was observed that rSaeno was actually very stable in the presence of Mg^{2+}, Zn^{2+} and Mn^{2+} (figure 8). Intrinsic tryptophan fluorescence was employed to analyse the alterations in the proteins' architecture on incubation with various divalent cations (Mg^{2+}, Zn^{2+}, Mn^{2+}, Cu^{2+}, Ni^{2+}, Ca^{2+}, NH_4^+ and Hg^{2+}). rSaeno emission spectra ranged from 325 to 330 nm with emission maxima (λ_{max}) at 328 nm. But, no significant shift in the emission maxima (λ_{max}) was observed on incubation with different cations. The emission intensity was maximum on incubation with Mg^{2+}, Zn^{2+}, Mn^{2+} and Cu^{2+} but the emission intensity decreased on incubation with other divalent cations (Ni^{2+}, Ca^{2+}, NH_4^+ and Hg^{2+}) (figure 9).

Table 3. Effect of divalent cations on reversible (acrylamide), and irreversible (2-5-H) inhibition of rSaeno

Inhibitor	% Inhibition of rSaeno activity by inhibitor	% Inhibition of rSaeno activity by inhibitor +1 mM Mg^{2+}	% Inhibition of rSaeno activity by inhibitor +1 mM Zn^{2+}	% Inhibition of rSaeno activity by inhibitor +1 mM Mn^{2+}
15 nM Acrylamide	65.0	42.0	63.0	79
2 mM 2,5-Hexanedione	44.1	43.80	71.92	80.70
10 mM 2,5-Hexanedione	100.0	90.1	95.3	99.1

15 nM rSaeno was initially preincubated with various divalent cations (1 mM Mg^{2+}, 1 mM Zn^{2+} or 1 mM Mn^{2+}) in 20 mM Tris-HCl (pH 7.5) and then further incubated with the inhibitors separately (15 nM acrylamide, 2 mM 2,5-hexanedione or 10 mM 2,5-hexanedione). At the end of the incubation, 400 mM KCl and 2 mM PEP were added. Then, decrease in the absorbance of PEP at 240 nm was monitored for 15 min at 1 s intervals at 25 ± 1°C.

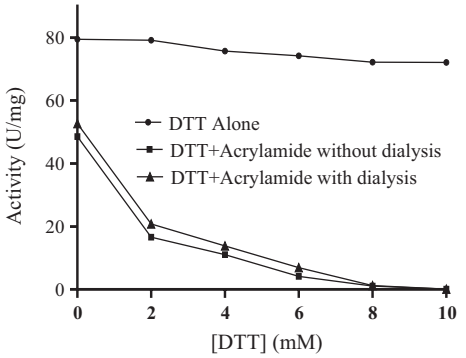

Figure 5. Inhibitory effect of acrylamide on rSaeno in the presence of DTT. The effect of DTT (0–10 mM) alone on rSaeno activity was determined in standard assay buffer (20 mM Tris-HCl (pH 7.5), 1 mM $MgSO_4$, 400 mM KCl and 15 nM rSaeno). The reaction was initiated by the addition of 2 mM PEP. The absorbance of PEP at 240 nm was monitored for 15 min at 1 s intervals at 25 ± 1°C. Further, 15 nM of rSaeno and 15 nM of acrylamide were preincubated with various concentrations of DTT (0–10 mM) and the effect of DTT on acrylamide inhibition of rSaeno was studied. DTT–acrylamide–rSaeno inhibitory complex was dialysed and the dialysed enzyme was assayed in the standard assay buffer at 240 nm for 15 min at 1 s intervals to determine the reversibility of DTT-mediated acrylamide inhibition of rSaeno.

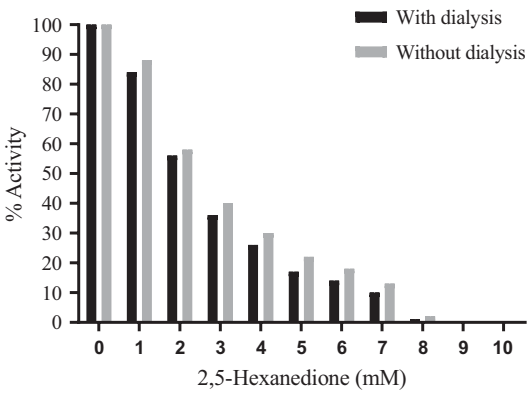

Figure 6. Inhibitory effects of 2,5-hexanedione on rSaeno activity. 15 nM rSaeno was assayed in the presence of increasing concentrations of 2,5-hexanedione (0–10 mM) in standard assay buffer (400 mM KCl, 1 mM $MgSO_4$ and 15 nM rSaeno). The reaction was initiated by the addition of 2 mM PEP. The absorbance of PEP at 240 nm was monitored for 15 min at 1 s intervals at 25 ± 1°C. To analyse the reversibility of 2,5-hexanedione inhibition, the 2,5-hexanedione–rSaeno complex was dialysed and the dialysed enzyme was analysed for rSaeno activity in the standard assay buffer at 25 ± 1°C.

3.11 *Mg^{2+} provided the most stable rSaeno conformation*

Limited or partial trypsin digestion was employed to determine the stability and gross similarity/dissimilarity of rSaeno conformation in the presence of different divalent cations (Mg^{2+}, Zn^{2+}, Mn^{2+}, Cu^{2+}, Ni^{2+} and Hg^{2+}). The

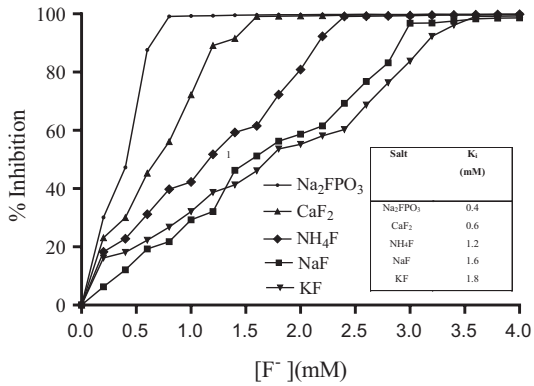

Salt	K_i (mM)
Na_2FPO_3	0.4
CaF_2	0.6
NH_4F	1.2
NaF	1.6
KF	1.8

Figure 7. Fluoride inhibition of rSaeno. To the standard assay mixture (20 mM Tris-HCl (pH 7.5), 400 mM KCl, 1 mM $MgSO_4$ and 15 nM rSaeno), varying concentrations (0–5 mM) of Na_2FPO_3, NaF, CaF_2, KF and NH_4F were added individually. The reaction was initiated by the addition of 2 mM PEP and the decrease in the absorbance of PEP at 240 nm was monitored for 15 min at 1 s intervals at 25 ± 1°C. The inhibitor concentration at half-maximal inhibition was considered as inhibitory constant (K_i).

summarized result of this experiment is depicted in figure 10A–C. In the present study, rSaeno was almost completely digested upon incubation with trypsin and EDTA (83% in 5 min and 99% in 15 min), but the replacement of EDTA with divalent cations conferred certain levels of protection against trypsin digestion. Zn^{2+} provided 78%, Mn^{2+} gave 54% and Cu^{2+} provided 40% protection in 5 min duration but failed to provide prolonged protection as the protection percentage decreased to 42, 17 and 0.8% respectively upon 15 min of incubation. In line with this, Mg^{2+} provided maximum and prolonged protection (87% in 5 min and 70% in 15 min). While Ni^{2+} and Hg^{2+} were the poorest in protection. Ni^{2+} gave 8% and Hg^{2+} gave 5% protection in 5 min duration and provided 0.7% protection and 0.5% protection respectively upon 15 min incubation. This indicates that Mg^{2+} maintains rSaeno in the most stable conformation (figure 10A–C).

4. Discussion

In the present study, *S. aureus* enolase was cloned, overexpressed, purified and characterized as a histidine-tagged recombinant enzyme (rSaeno). rSaeno has been purified to homogeneity (supplementary data 1, 2, 3 and 4) and it can successfully catalyse the conversion of PEP into 2-PGA. The calculated subunit molecular mass of rSaeno is 48.181 Da, which is in close resemblance to the enolase from other organisms such as *Leuconostoc mesenteroides* 47 kDa (Lee *et al.* 2006), *E. coli* enolase 46 kDa (Wold and Ballou 1957) and carp muscle enolase 49 kDa (Pietkiewicz *et al.* 1983). In this study with rSaeno, the K_m for PEP was $0.231 \pm 0.013 \times 10^{-3}$ M and V_{max} was 90.98 ± 0.00052 U/mg (figure 1). Thus, the special feature of *S. aureus* enolase which markedly differentiates it from the enolases of

Table 4. Effect of divalent cations on quasi-irreversible (fluoride) inhibition of rSaeno

	Percentage inhibition		
Na_2FPO_3 (mM)	Mg^{2+} (1 mM)	Zn^{2+} (1 mM)	Mn^{2+} (1 mM)
0	0	0	0
0.2	30.1	9.8	3.8
0.4	47.3	31.4	12.7
0.6	87.6	66.9	53.8
0.8	99.5	82.3	68.2

15 nM rSaeno inhibition in various concentrations of sodium fluorophosphate (Na_2FPO_3) (0–5 mM) was assayed in the presence of 1 mM sulphates of magnesium, manganese and zinc.

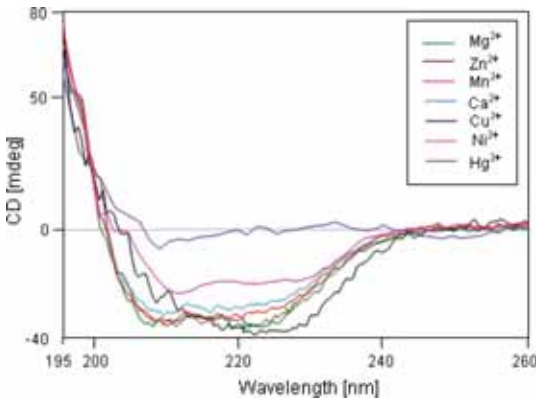

Figure 8. Far UV-CD spectrum of rSaeno in the presence of different metals; rSaeno was preincubated with buffers containing different metal ions (Mg^{2+}, Zn^{2+}, Mn^{2+}, Cu^{2+}, Ca^{2+}, Ni^{2+} or Hg^{2+}) for 15 min and the resulting variations in secondary structures were analysed by CD (wavelength 200–260 nm).

Table 5. The percentage variations in secondary structural components of rSaeno induced by different metal ions

Metal ions	α-Helix (%)	β-Sheet (%)	Turn (%)	Random coil (%)
Mg^{2+}	40.4	33.6	13.2	12.8
Zn^{2+}	40.3	30.3	12.7	16.7
Mn^{2+}	39.6	26.7	13.1	20.6
Cu^{2+}	28.6	0.0	31.0	40.4
Ca^{2+}	34.7	21.9	14.3	29.1
Ni^{2+}	31.1	0.0	25.8	43.1
Hg^{2+}	12.1	0.0	24.8	63.1

rSaeno was pre-incubated with different ions (Mg^{2+}, Zn^{2+}, Mn^{2+}, Cu^{2+}, Ni^{2+}, Ca^{2+} and Hg^{2+}) for 15 min and was subjected to CD analysis. The table demonstrates the percentage variations in secondary structural components due to varying metal ion treatments.

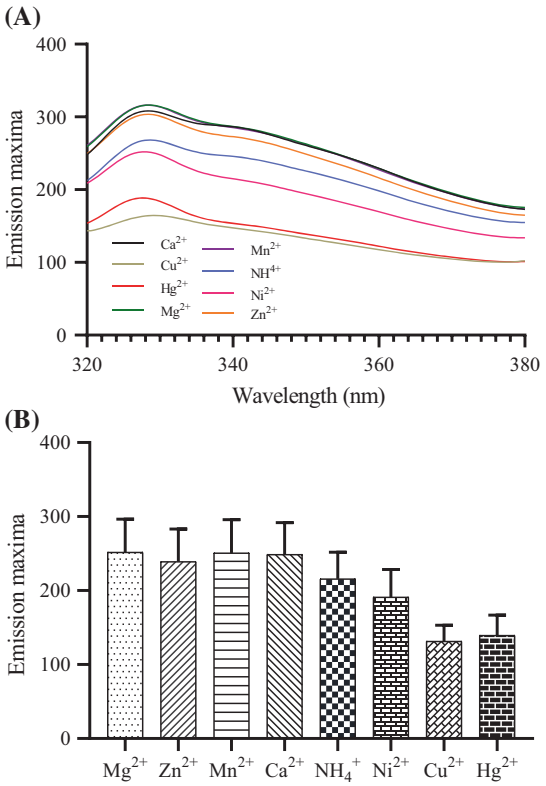

Figure 9. Intrinsic tryptophan fluorescence (λ_{ex} at 295 nm) for determination of variations in the protein architecture due to the effect of metal ions (Mg^{2+}, Zn^{2+}, Mn^{2+}, Cu^{2+}, Ni^{2+}, Ca^{2+} and Hg^{2+}). rSaeno was incubated with buffers of different metal ions (Mg^{2+}, Zn^{2+}, Mn^{2+}, Cu^{2+}, Ca^{2+}, Ni^{2+} and Hg^{2+}) for 15 min. The intrinsic tryptophan fluorescence was monitored at 25 ± 1°C on a JASCO FP8200 spectrofluorimeter.

other organisms is that the former can catalyse the reverse reaction (PEP to 2-PGA) very efficiently (Agarwal *et al.* 2008). Monovalent cations were found to have a profound impact on rSaeno activity. Higher concentrations of Na^+ inhibited the catalysis whereas K^+ stimulated the activity (Pal-Bhowmick *et al.* 2004). However, the activation induced by K^+ ions depends on the source of enolase; for example, in yeast enolase, K^+ was neutral in reactivity but in rabbit enolase and rSaeno the K^+ activated the catalysis (Kornblatt and Klugerman 1989). But, the negligible impact on structural integrity indicates that these monovalent cations alter the reaction mechanisms of rSaeno (supplementary figures 5 and 6).

Enolase can bind three metal ions per subunit in its conformational, catalytic and inhibitory site, respectively. The metal ion initially binds to the conformational site and induces the modification in the active site and initiates the binding of substrate. Upon binding of the substrate, the divalent cations bind to the catalytic site and initiate the reaction (Han *et al.* 2012; Wu *et al.* 2015). The substrate binding and catalytic cation binding are synergistic. However, at higher concentrations, the divalent cations bind to the inhibitory site and inhibit the activity of enolase (Brewer 1981; 1985). In the present study, rSaeno exhibits the highest catalytic activity as well as the most stable secondary structure in the presence of Mg^{2+}, Zn^{2+} and Mn^{2+}. Possibly,

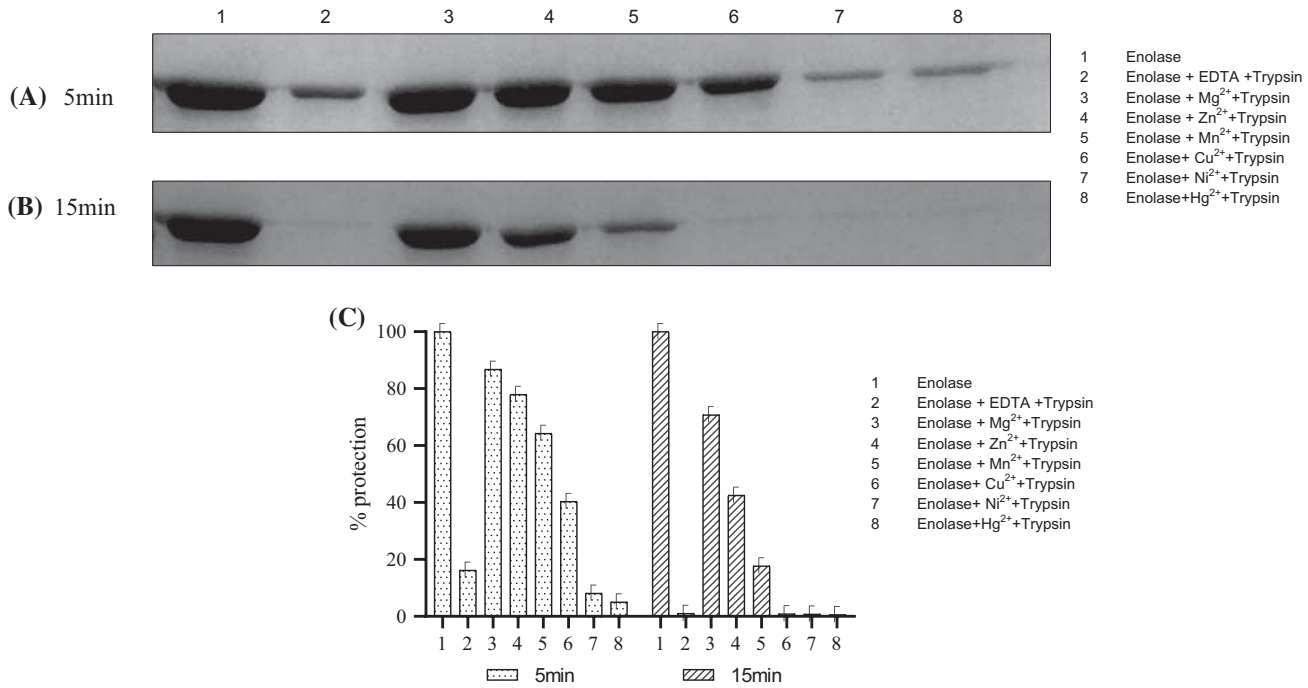

Figure 10. Comparison of conformational states of rSaeno using limited trypsin digestion. (**A**) Lane 1 is 0.5 mg/mL of rSaeno in 50 mM Tris-HCl, pH 7.5. Lane 2 is 0.5 mg/mL rSaeno with 0.001 mg/mL trypsin and 2 mM EDTA. Lane 3 is 0.5 mg/mL rSaeno with 0.001 mg/mL trypsin and 5 mM Mg^{2+}. Lane 4 is 0.5 mg/mL rSaeno with 0.001 mg/mL trypsin and 5 mM Zn^{2+}. Lane 5 is 0.5 mg/mL rSaeno with 0.001 mg/mL trypsin and 5 mM Mn^{2+}. Lane 6 is 0.5 mg/mL rSaeno with 0.001 mg/mL trypsin and 5 mM Cu^{2+}. Lane 7 is 0.5 mg/mL rSaeno with 0.001 mg/mL trypsin and 5 mM Ni^{2+}. Lane 8 is 0.5 mg/mL rSaeno with 0.001 mg/mL trypsin and 5 Mm Hg^{2+}. These reaction mixtures were incubated for 5 (**A**) and 15 min (**B**) and ran on SDS-12% PAGE. The quantification of undigested bands was carried out by using ImageJ and is plotted in (**C**). Lane 1 was considered to be 100% for determining the undigested fractions of rSaeno in trypsin treated samples (lanes 2, 3, 4 and 5).

these activating metal ions bound to the conformational site of the protein and facilitated the conversion of PEP into 2-PGA (Brewer 1981; Han *et al.* 2012). However, at higher concentrations, these metals might have bound to the inhibitory site of rSaeno and resulted in the reduced catalytic activity of rSaeno.

These observations indicate that the catalytic activity of rSaeno (at a different ion) might stem from its biological structure. To further test this hypothesis, the CD spectra (200–260 nm) of rSaeno under different conditions were studied. According to the CD spectra, other than Hg^{2+}, Ni^{2+} and to a certain extent Cu^{2+}, none of the other ions destabilized rSaeno. And the rSaeno was structurally very stable in Mg^{2+}, Zn^{2+} and Mn^{2+}.

Enolase catalysis can be divided into three separate steps: proton abstraction, hydroxyl ion removal and product release (Shen and Westhead 1973; Vinarov and Nowak 1998). The proton abstraction is very slow in any pH lower than the optimum pH; however, at a pH higher than optimum pH, the hydroxyl ion removal and product release are hindered. The divalent cations other than Mg^{2+} were ineffective at catalysis due to the incapability in hydroxyl group removal or product release (Brewer 1981; Lee and Nowak 1992). In agreement with this, the optimum activity of rSaeno was observed at pH 7.5 in the presence of Mg^{2+}, and any changes in the pH above or below the optimum pH, there was a drastic decrease in the activity of rSaeno.

Acrylamide inhibits both neuronal and non-neuronal enolase. In the case of rSaeno the inhibition followed the Michaelis–Menten kinetics plot, and it is very clear that upon acrylamide inhibition the K_m increased and V_{max} decreased, indicating the mixed type of inhibition (Howland *et al.* 1980).

To analyse the reversibility of acrylamide inhibition, the enzyme–inhibitor complex was dialysed and it was found that the enzyme regained its catalytic ability. It shows that the inhibition was reversible. But in the presence of reducing agents such as DTT, there was an augmentation in the inhibition. But DTT alone failed to inhibit rSaeno (Howland *et al.* 1980; Sabri 1983). As it is evident from figure 5, there is a sharp decrease in rSaeno activity as the DTT concentration is increased. To analyse the impact of DTT on the reversibility of the inhibition, acrylamide and DTT inhibitory complex was dialysed; but there was no reactivation of enolase activity at the end of the dialysis. rSaeno lacks the S–S– bond; this probably accounts for the inability of DTT to inhibit the reaction catalysed by rSaeno (figure 5). However, somehow DTT enhances the acrylamide inhibition of rSaeno.

Our initial analysis clearly indicates that 2,5-hexanedione inhibition was independent of preincubation. Moreover, the inhibition is dose-dependent. The dialysis of the enolase-2,5-hexanedione inhibitory complex was not effective at rejuvenating the enolase activity, indicating the irreversible nature of inhibition. The irreversibility is possibly due to the covalent interaction between 2,5-hexanedione and rSaeno active site residues (Wold 1971; Howland *et al.* 1980).

It is very much clear from table 5 that Mg^{2+} confers maximum protection as compared with Zn^{2+} or Mn^{2+} in the acrylamide inhibition. This is mainly because Mg^{2+} binds both conformational and catalytic site of enolase considerably with more affinity in comparison with Zn^{2+} or Mn^{2+}. Therefore, inhibition in the presence of Mg^{2+} resulted in the formation of a more stable closed form of the enzyme which favours substrate binding. This induces the event of cooperative binding of catalytic cations to enolase, eventually leading to having some considerable amount of reaction, even in the presence of an inhibitor (Brewer and Weber 1966; Wold 1971; Faller and Johnson 1974; Brewer 1985). On the other hand, Zn^{2+} or Mn^{2+} ions were unable to form such stable closed conformation of enolase thereby rendering the enolase in an open conformation which favours acrylamide inhibition. Therefore, there was a significant increment in acrylamide inhibition when Mg^{2+} was replaced with Zn^{2+} or Mn^{2+}.

The above-mentioned metal-induced protective mechanism seems to be functional only in reversible inhibition. But in the irreversible inhibition, where covalent interactions are employed for inhibition, the metal ions were unable to confer any kind of protective effect towards inhibition (Brewer 1981, 1985; Lee and Nowak 1992). As has already been observed in the case of 2,5-hexanedione-mediated inhibition, the enolase catalytic efficiency was not protected due to preincubation with any divalent cations including the most potent natural metal ions such as Mg^{2+} (table 3) (Brewer and Weber 1966; Wold 1971).

It is well understood that fluoride inhibits the glycolytic pathway by inhibiting one of the prime glycolytic enzymes enolase. The inhibition is mainly due to the formation of the magnesium fluoride complex (Lebioda *et al.* 1993). Interestingly, in the presence of phosphate, the inhibition is significantly enhanced. This suggests that fluoride and phosphate cooperatively bind to the enolase (Wang and Himoe 1974; Lebioda *et al.* 1993). More specifically, fluoride coordinates with magnesium and this complex is more stabilized by phosphate. Hence, sodium fluorophosphates inhibited rSaeno more strongly (figure 7). One fluoride ion binds per subunit of the enzyme, and it specifically binds to the magnesium ion in the conformational site as well as phosphate. Another fluoride ion binds only to catalytic Mg^{2+} upon binding of the substrate (Lebioda *et al.* 1993; Belli *et al.* 1995; Qin *et al.* 2006).

Wang and Himoe showed that magnesium-activated enolase is more strongly inhibited by fluoride. The replacement of Mg^{2+} with Mn^{2+} resulted in a 40% decrease in the inhibition while Zn^{2+} led to no inhibition (Wang and Himoe 1974). But in the present study, the maximum inhibition was observed in the presence of Mg^{2+} and when Mg^{2+} was replaced with Mn^{2+} there was 30% reduction in the inhibition and in the case of Zn^{2+}, there was 20% decrease in the inhibition.

The binding of conformational cation induces the enolase to attain the closed conformation which favours the binding of catalytic cations and substrate. The crystal structure of yeast enolase indicated that closed conformation of enolase is more favourable for the binding of negatively charged ligands such as fluoride and phosphate (Wang and Himoe 1974; Lebioda *et al.* 1993; Guha-Chowdhury *et al.* 1997).

The fluoride inhibition is reversible in the absence of phosphate. Fluoride competes with the substrate to bind to the catalytic site. But in the presence of phosphate, the fluoride inhibition is irreversible. Therefore, the fluoride inhibition is termed as quasi-irreversible inhibition (Lebioda *et al.* 1993; Curran *et al.* 1994; Belli *et al.* 1995).

Native enolase mainly exists as an inactive open conformational apoprotein (Dutta *et al.* 2015). The binding of divalent cations induces the conformational changes in enolase to attain stable, catalytically active closed conformation. Many studies have shown that Mg^{2+} gives maximum structural stability and catalytic efficiency because the enolase can attain a properly closed conformation in the presence of Mg^{2+}. The stability of closed conformation can be reduced when Mg^{2+} is replaced with other divalent cations such as Mn^{2+} or Zn^{2+} (Brewer and Weber 1966; Wold 1971; Dutta *et al.* 2015). To elucidate the impact of different divalent cations on the ability of rSaeno to form a structurally stable closed conformation, the enzyme was incubated with Mg^{2+}, Zn^{2+}, Mn^{2+}, Cu^{2+}, Ni^{2+} and Hg^{2+}. The maximum protection was observed in the case of enolase preincubated with Mg^{2+}, as it prevented trypsin-mediated proteolysis. Apoenolase which was in open inactive conformation was more susceptible to trypsin digestion but there were increments in the resistance towards trypsin digestion on incubation with Mg^{2+} which converted open inactive conformation into active closed conformation. But other metals were unable to provide as much protection as Mg^{2+} because the stability of closed conformation was compromised due to changes in divalent cations (Dutta *et al.* 2015).

5. Conclusions

Increasing concentrations of Na^{+} ions inhibit rSaeno while increasing concentrations of K^{+} ions were stimulatory. rSaeno was catalytically very efficient and structurally very stable in the presence of Mg^{2+}, Zn^{2+} and Mn^{2+}. However, higher concentrations of divalent cations were inhibitory for rSaeno activity. The optimum pH for rSaeno was 7.5. Neurotoxins such as acrylamide reversibly inhibited rSaeno, whereas 2,5-hexanedione irreversibly inhibited rSaeno.

Divalent cations were unable to confer any protection in the irreversible inhibition. rSaeno attained a very stable conformation in the presence of Mg^{2+}. Sodium fluorophosphate is the potent inhibitor of rSaeno, the inhibition was potentiated by Mg^{2+} and phosphate.

Acknowledgements

This work was supported by the financial assistance from DST, Govt. of India to Dr Malabika Biswas (Sanction No. EMR/2015/002229). Mr Vijay Hemmadi is a recipient of Junior Research Fellowship from DST, Govt. of India. Mr Avijit Das is a recipient of Institute Fellowship from BITS-Pilani, K. K. Birla Goa campus.

References

Agarwal S, Kulshreshtha P, Mukku DB and Bhatnagar R 2008 α-Enolase binds to human plasminogen on the surface of *Bacillus anthracis*. *Biochim. Biophys. Acta, Proteins Proteomics* **1784** 986–994

Barnes LD and Stcllwagen E 1973 Enolase from the thermophile *Thermus X-l. Biochemistry* **12** 1559–1565

Belli WA, Buckley DH and Marquis RE 1995 Weak acid effects and fluoride inhibition of glycolysis by *Streptococcus* mutans GS-5. *Can. J. Microbiol.* **41** 785–791

Brewer JM 1981 Yeast enolase: Mechanism of activation by a metal ion. *Crit. Rev. Biochem.* **11** 209–254

Brewer JM 1985 Specificity and mechanism of action of metal ions in yeast enolase. *FEBS Lett.* **182** 8–14

Brewer JM and Weber G 1966 The effect of magnesium on some physical properties of yeast enolase. *J. Biol. Chem.* **16** 3864–3869

Brown CK, Kuhlman PL, Mattingly S, Slates K, Calie PJ and Farrar WW 1998 A model of the quaternary structure of enolases, based on structural and evolutionary analysis of the octameric enolase from *Bacillus subtilis*. *J. Protein Chem.* **17** 855–866

Carneiro CR, Postol E, Nomizo R, Reis LF and Brentani RR 2004 Identification of enolase as a laminin-binding protein on the surface of *Staphylococcus aureus*. *Microbes Infect.* **6** 604–608

Chambers HF 2001 The changing epidemiology of *Staphylococcus aureus*? *Emerg. Infect. Dis.* **7** 178–182

Curran TM, Buckley DH and Marquis RE 1994 Quasi-irreversible inhibition of enolase of *Streptococcus* mutans by flouride. *FEMS Microbiol. Lett.* **119** 283–288.

Dutta S, Mukherjee D and Jarori GK 2015 Replacement of Ser108 in *Plasmodium falciparum* enolase results in weak Mg[II] binding: Role of a parasite-specific pentapeptide insert in stabilizing the active conformation of the enzyme. *FEBS J.* **282** 2296–2308

Ehinger S, Schubert WD, Bergmann S, Hammerschmidt S and Heinz DW 2004 Plasmin [ogen]-binding α-enolase from *Streptococcus pneumoniae*: Crystal structure and evaluation of plasmin [ogen]-binding sites. *J. Mol. Biol.* **343** 997–1005

Faller LD and Johnson AM 1974 Calorimetric studies of the role of magnesium ions in yeast enolase catalysis. *Proc. Natl. Acad. Sci. USA* **71** 1083–1087

Guha-Chowdhury N, Clark AG and Sissons CH 1997 Inhibition of purified enolases from oral bacteria by fluoride. *Mol. Oral. Microbiol.* **12** 91–97

Han X, Ding C, Chen H, Hu Q and Yu S 2012 Enzymatic and biological characteristics of enolase in *Brucella abortus* A19. *Mol. Biol. Rep.* **39** 2705–2711

Howland RD, Vyas IL, Lowndes, HE and Argentieri TM 1980 The etiology of toxic peripheral neuropathies: *In vitro* effects of acrylamide and 2,5-hexanedione on brain enolase and other glycolytic enzymes. *Brain Res.* **202** 131–142

Kornblatt MJ and Klugerman A 1989 Characterization of the enolase isozymes of rabbit brain: Kinetic differences between mammalian and yeast enolases. *Biochem. Cell Biol.* **67** 103–107

Lebioda L, Zhang E, Lewinski K and Brewer JM 1993 Fluoride inhibition of yeast enolase: Crystal structure of the enolase–Mg^{2+}–F–Pi complex at 2.6 Å resolution. *Proteins: Struct., Funct., Bioinf.* **16** 219–225

Lee BH and Nowak T 1992 Influence of pH on the manganese[2+] activation of and binding to yeast enolase: A functional study. *Biochemistry* **31** 2165–2171

Lee CY and Iandolo JJ 1988 Structural analysis of *staphylococcal* bacteriophage phi 11 attachment sites. *J. Bacteriol.* **170** 2409–2411

Lee JH, Kang HK, Moon YH, Cho DL, Kim D, Choe JY and Robyt JF 2006 Cloning, expression, and characterization of an extracellular enolase from *Leuconostoc mesenteroides*. *FEMS Microbiol. Lett.* **259** 240–248

Lu Q, Lu H, Qi J, Lu G and Gao GF 2012 An octamer of enolase from *Streptococcus suis*. *Protein Cell* **3** 769–780

Maurer PJ and Nowak T 1981 Fluoride inhibition of yeast enolase. 1. Formation of the ligand complexes. *Biochemistry* **20** 6894–6900

Pal-Bhowmick I, Sadagopan K, Vora HK, Sehgal A, Sharma S and Jarori GK 2004 Cloning, overexpression, purification and characterization of *Plasmodium falciparum* enolase. *FEBS J.* **271** 4845–4854

Pancholi V 2001 Multifunctional α-enolase: Its role in diseases. *Cell. Mol. Life Sci. CMLS* **58** 902–920

Pietkiewicz J, Kustrzeba-Wójcicka Irena and Wolna EB 1983 Purification and properties of enolase from carp [*Cyprinus carpio*]. Comparison with enolases from mammals' muscles and yeast. *Comp. Biochem. Physiol., B* **75** 693–698

Proctor RA 2012 Is there a future for a *Staphylococcus aureus* vaccine? *Vaccine* **30** 2921–2927

Qin J, Chai G, Brewer JM, Lovelace, LL and Lebioda L 2006 Fluoride inhibition of enolase: Crystal structure and thermodynamics. *Biochemistry* **45** 793–800

Raghunathan K, Harris PT, Spurbeck RR, Arvidson CG and Arvidson DN 2014 Crystal structure of an *efficacious gonococcal* adherence inhibitor: An enolase from *Lactobacillus gasseri*. *FEBS Lett.* **588** 2212–2216

Sabri MI 1983 *In vitro* and *in vivo* inhibition of glycolytic enzymes by acrylamide. *Neurochem. Pathol.* **1** 179–191

Sambrook J, Fritsch EF and Maniatis T 1989 *Molecular cloning. A laboratory manual*, vol. **1** (NY: Spring Harbor Laboratory Press, Cold Spring Harbor) pp. 1339–1341

Shen TY and Westhead EW 1973 Divalent cation and pH-dependent primary isotope effects in the enolase reaction. *Biochemistry* **13** 3292–3297

Sreerama N and Woody RW 2000 Estimation of protein secondary structure from circular dichroism spectra: Comparison of CONTIN, SELCON, and CDSSTR methods with an expanded reference set. *Anal. Biochem.* **287** 252–260

Steinberg JP, Clark CC and Hackman BO 1996 Nosocomial and community-acquired *Staphylococcus aureus* bacteremias from 1980 to 1993: Impact of intravascular devices and methicillin resistance. *Clin. Infect. Dis.* **23** 255–225

Vinarov DA and Nowak T 1998 pH dependence of the reaction catalyzed by yeast Mg-enolase. *Biochemistry* **37** 15238–15246

Wang T and Himoe A 1974 Kinetics of the rabbit muscle enolase-catalyzed dehydration of 2-phosphoglycerate fluoride and phosphate inhibition. *J. Biol. Chem.* **249** 3895–3902

Wold F 1971 18 enolase; in *The enzymes* vol. **5** (Academic Press) pp. 499–538

Wold F and Ballou CE 1957 Studies on the enzyme enolase I. Equilibrium studies. *J. Biol. Chem.* **227** 301–312

Wu Y, Wang C, Lin S, Wu M, Han L, Tian C and Zang J 2015 Octameric structure of *Staphylococcus aureus* enolase in complex with phosphoenolpyruvate. *Acta Crystallogr., Sect. D: Biol. Crystallogr.* **71** 2457–2470

Zhao J, Carmody LA, Kalikin LM, Li J, Petrosino JF, Schloss PD and LiPuma JJ 2012 Impact of enhanced *Staphylococcus* DNA extraction on microbial community measures in cystic fibrosis sputum. *PLoS One* **7** e33127

Corresponding editor: Saumitra Das